

# **AOARD Research Project Report:**

**FA4868-08-1-4100 (AOARD-08-4100)**

---

## **Surface-Plasmon Enhanced Organic thin-film solar cells**

**Principle Investigator: Dr. Yun-Chorng Chang**

National Cheng Kung University  
Institute of Electro-Optical Science & Engineering  
No. 1 Ta-Hsueh Road, Tainan 701, Taiwan

## Report Documentation Page

*Form Approved*  
*OMB No. 0704-0188*

Public reporting burden for the collection of information is estimated to average 1 hour per response, including the time for reviewing instructions, searching existing data sources, gathering and maintaining the data needed, and completing and reviewing the collection of information. Send comments regarding this burden estimate or any other aspect of this collection of information, including suggestions for reducing this burden, to Washington Headquarters Services, Directorate for Information Operations and Reports, 1215 Jefferson Davis Highway, Suite 1204, Arlington VA 22202-4302. Respondents should be aware that notwithstanding any other provision of law, no person shall be subject to a penalty for failing to comply with a collection of information if it does not display a currently valid OMB control number.

1. REPORT DATE <b>04 FEB 2010</b>	2. REPORT TYPE <b>FInal</b>	3. DATES COVERED <b>22-05-2008 to 21-05-2009</b>	
4. TITLE AND SUBTITLE <b>Surface-plasmon-enhanced organic thin-film solar cells</b>		5a. CONTRACT NUMBER <b>FA48690814100</b>	
		5b. GRANT NUMBER	
		5c. PROGRAM ELEMENT NUMBER	
6. AUTHOR(S) <b>Yia-Chung Chang</b>		5d. PROJECT NUMBER	
		5e. TASK NUMBER	
		5f. WORK UNIT NUMBER	
7. PERFORMING ORGANIZATION NAME(S) AND ADDRESS(ES) <b>Academia Sinica,128 Section 2, Academia Rd,Nankang 11529,Taiwan,TW,11529</b>		8. PERFORMING ORGANIZATION REPORT NUMBER <b>N/A</b>	
9. SPONSORING/MONITORING AGENCY NAME(S) AND ADDRESS(ES) <b>AOARD, UNIT 45002, APO, AP, 96337-5002</b>		10. SPONSOR/MONITOR'S ACRONYM(S) <b>AOARD</b>	
		11. SPONSOR/MONITOR'S REPORT NUMBER(S) <b>AOARD-084100</b>	
12. DISTRIBUTION/AVAILABILITY STATEMENT <b>Approved for public release; distribution unlimited</b>			
13. SUPPLEMENTARY NOTES			
14. ABSTRACT <b>The effects of surface plasmon on the performance of organic solar cells were investigated. Metallic nanoparticles fabricated using thermal anneal and Nanosphere lithography wereh experimentally and theoretically studied to understand their corresponding surface plasmon resonance. Near-field Scanning Optical Microscopy (NSOM) was used to investigate the strength of the optical near-field that is very close to the metal nanoparticles when illuminated with light that was resonant to the metal nanoparticles. NSOM measurements revealed great electric fields created due to the effects of surface plasmon of metal nanoparticles. Integration of selected metal nanoparticles and organic thin film were investigated. Further investigation of the plasmonic-enhanced photonic devices is emphasized as future goal as well as the development of Nanosphere lithography. A fast and economic nanofabrication technique will find a suitable application in the optoelectronic industry. The results from this research will greatly improve the understanding of the plasmonic-enhanced photonic devices and find new application in the development of future technologies.</b>			
15. SUBJECT TERMS <b>Solar Cells, Polymer Thin Films, Nano-lithography</b>			
16. SECURITY CLASSIFICATION OF:			17. LIMITATION OF ABSTRACT <b>Same as Report (SAR)</b>
a. REPORT <b>unclassified</b>	b. ABSTRACT <b>unclassified</b>	c. THIS PAGE <b>unclassified</b>	
			18. NUMBER OF PAGES <b>14</b>
			19a. NAME OF RESPONSIBLE PERSON

## **Contents**

<b>I. Abstract .....</b>	<b>3</b>
<b>II. Technical milestones .....</b>	<b>4</b>
<b>III. Summary of Accomplishments .....</b>	<b>5</b>
<b>IV. Enhanced near-field imaging contrasts of silver nanoparticles by localized surface plasmon.....</b>	<b>6</b>
<b>V. Future work .....</b>	<b>13</b>
<b>VI. Conclusions .....</b>	<b>14</b>

## **I. Abstract**

The effects of surface plasmon on the performance of organic solar cells were investigated. Metallic nanoparticles fabricated using thermal anneal and Nanosphere lithography were both experimentally and theoretically studied to understand their corresponding surface plasmon resonance. Near-field Scanning Optical Microscopy (NSOM) were used to investigated the strength of the optical near-field that is very close to the metal nanoparticles when illuminated with light that was resonant to the metal nanoparticles. NSOM measurements revealed great electric fields were presented due to the effects of surface plasmon of metal nanoparticles. Integration of selected metal nanoparticles and organic thin film were currently under investigation. The further investigation of the plasmonic-enhanced photonic devices will be emphasized as the short-term future goal as well as the development of Nanosphere lithography. The fast and economic nanofabrication technique should be able to find a suitable application in the optoelectronic industry. The results from this research will greatly improved the understanding of the plasmonic-enhanced photonic devices and find new application in the development of future technologies.

## **II. Technical milestones**

### **Milestone 1: Fabrications of two-dimensional metal nanoparticle arrays**

Fabricate two-dimensional metal nanoparticle arrays were achieved both by thermal annealing and Nanosphere Lithography techniques, which are both very fast and economic. The surface plasmon resonance of the fabricated nanostructure was analyzed experimentally by optical absorption spectroscopy and theoretically by three-dimensional finite-difference time-domain calculation. The surface plasmon resonance frequency of the metal nanostructure can be modified to match the solar spectrum by adjusting several processing parameters. These results will provide will provide the science community with the database of the surface plasmon resonance of different metal nanoparticles arrays with different sizes and shapes.

### **Milestone 2: Nanoscale-optical characterization of the plasmonic effects**

Nanoscale-optical characterization of the metal nanoparticles was performed using near-field scanning optical microscopy (NSOM) and the effects of the surface plasmon were studied. Tapped fiber scanning tip were used to investigate the near-field electric field and coupling the near-field light to the far-field and detected by conventional light detecting setup. Strong near-field electric field was detected near the metal nanoparticle when using light that matches the surface plasmon resonance of the metal nanoparticles. The induced high electric field only exist at the metal-dielectric interface and decay exponential rapidly when moving away from the interface. Therefore, the optical absorption should be greatly enhanced near the metal nanoparticles. The scientific impact of these measurements provided necessary evidences to answer whether effects of surface plasmon can be used to enhance the power conversion efficiency.

### **Milestone 3: The implementation of the metal nanoparticle array into the design of organic solar cells.**

The metal nanoparticles arrays were fabricated on top of transparent conducting oxides (ITO). A standard organic solar cell was subsequently fabricated on top of the array. The metal and the organic layer were very close and the plasmonic effects can enhance the optical absorption. Standard Incident photon-to-current conversion efficiency (IPCE) measurements were performed to determine the plasmonic effects on the conversion efficiency at different optical wavelengths. An organic thin-film solar cell with enhanced conversion efficiency is expected in this study.

### III. Summary of Accomplishments

1. **"Enhanced near-field imaging contrasts of silver nanoparticles by localized surface plasmon", *IEEE Journal Selected Topics in Quantum Electronics* **14**, 1536 (2008). (AOARD-08-4100) SCI: 2.518**
2. **"Sub-bandgap laser light-induced excess carrier transport between surface states and two-dimensional electron gas channel in AlGaIn/GaN structure", *IEEE Journal of Quantum Electronics* **46**, 112 (2010). (AOARD-08-4100) SCI: 2.413**

## **IV. Enhanced near-field imaging contrasts of silver nanoparticles by localized surface plasmon**

### **INTRODUCTION**

Techniques of nanoparticle detection have improved significantly for the demands of unprecedented high resolution in nanotechnologies. Information about the spatial distribution and chemical identity of nanoparticles provide vital information for both nano- and bio-sciences. Among different mapping techniques, optical methods offer fast, non-invasive and highly sensitive detections for wide variety of materials. Various near-field imaging techniques have been developed to overcome the Abbe's diffraction limit and achieve sub-wavelength spatial resolution [1-4]. In a recent report, material-specific particle recognition was achieved with sub-10 nm resolution due to the strong tip-substrate coupling in scattering type near-field scanning optical microscopy (NSOM) [5].

The detection sensitivities can be further enhanced by the effects of localized surface plasmon resonance (LSPR) from metallic nanoparticles. The collective resonant oscillation of the conduction electrons of metallic nanoparticles is the origin of localized surface plasmon. The LSPR frequencies depend strongly on the shapes and sizes of the nanoparticles as well as the dielectric environments [6]. LSPR spectrum of a single gold nanoparticle has been studied with the help of an aperture-type NSOM [7]. Similar results have also been reported using a scattering-type NSOM [8]. These reports indicated the potential of LSPR-assisted metallic nanoparticle imaging using NSOM technologies. However, the size dependence of the metallic nanoparticles and their corresponding NSOM images were not well-reported. In this study, near-field images of Ag nanoparticles with different sizes are studied using experimental NSOM measurements and 3-dimensional finite-difference-time-domain (FDTD) simulation. It is found that the transmitted intensity from the NSOM probe and the image contrast are greatly affected by the LSPR of the nanoparticle. The intensity contrast becomes highest when the wavelength of the incident light matches the LSPR of the nanoparticle. The enhancement factor is proportional to the resonant quality factor. This property can be useful to identify or grouping different size, shape and composites of particles on the same substrate.

## Experiments

Fabrications of Ag nanoparticle arrays were achieved by annealing 5 nm and 10 nm Ag thin films at 600 °C for 30 minute inside a nitrogen-flowing oven. Double-side-polished quartz substrates or silicon substrates were used for different subsequent analyses. Ag nanoparticles fabricated on top of silicon substrates were analyzed by a scanning electron microscopy (SEM). Fig 1(a) and 1(b) were SEM images of the Ag nanoparticles fabricated from 5 nm and 10 nm of Ag thin film on top of silicon substrates, respectively. The size distributions of Ag nanoparticles were subsequently analyzed from the SEM images and the results were shown in Fig. 1(c). The size and its variation are larger for Ag nanoparticles fabricated from thicker films. A commercial UV-VIS absorption spectrophotometer (Hitachi U-3010) was used to determine the surface plasmon resonance of the Ag nanoparticles, shown in Fig. 1(d). Samples for the absorption measurements were grown on top of transparent quartz substrates. The absorption spectrum from the Ag nanoparticles fabricated from 5 nm film, curve (a), exhibits an absorption peak centered at 440 nm. This peak is referred as the scattering peak from the Ag nanoparticles. Curve (b) is the absorption spectrum measured from Ag nanoparticles fabricated from 10 nm films and two peaks centered at

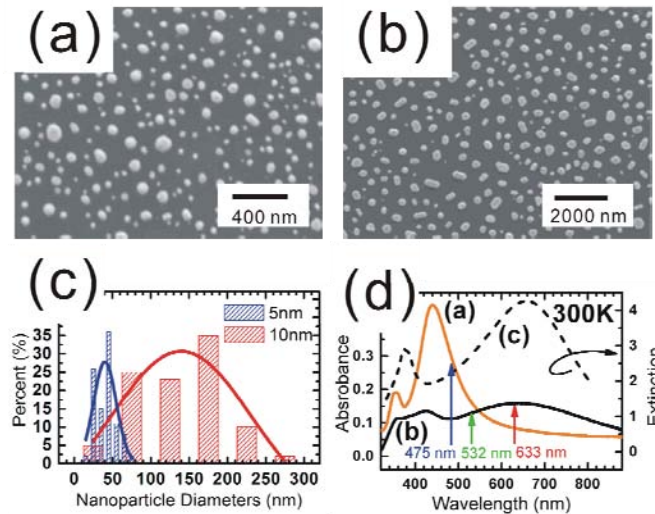


Fig. 1. SEM micrographs of (a) 5 nm and (b) 10 nm of Ag thin films annealed at 600°C for 30 minutes. (c) Distributions of Ag nanoparticle diameters and (d) absorption spectra for nanoparticles fabricated from 5 nm (curve a) and 10 nm (curve b) thin films. Curve c represents the calculated extinction spectrum for a 160 nm Ag nanoparticle from FDTD simulation. The blue, green, and red arrows in (d) indicates the laser wavelength used in this study.

420 nm and 630 nm are corresponding to the absorption and scattering peaks, respectively. The blue, green, and red arrows shown in Fig. 1(d) are the laser wavelength used in the subsequent near field measurements.

A commercial near-field scanning optical microscope scanner (Veeco Aurora-3) was used to obtain the near field images of the Ag nanoparticles. The probe tip was a tapered single mode fiber with an 80 nm aperture coated with 100 nm aluminum. Emission from a He-Ne laser ( $\lambda = 633$  nm) or frequency-doubled solid state lasers ( $\lambda = 475$  nm or 532 nm) was coupled into the other end of the tapered fiber. The NSOM was operated under the illumination mode and the transmitted light was collected in the far field by a microscope objective and analyzed by a photomultiplier.

### Results and discussion

NSOM images of Ag nanoparticles fabricated from 10 nm thin films are shown in Fig. 2. The topography image of the sample is shown in Fig. 2(a), and the NSOM images using 633 nm, 532 nm, and 475 nm laser light are shown in Fig. 2(b), (c), and (d), respectively. It should be noted that these lasers were with different emission intensities, and comparisons of the absolute transmitted intensities between different lasers were irrelevant. Only the intensity contrast between the signal from the nanoparticle and the background was discussed. Four nanoparticles are observed inside a high-lighted polygon area in Fig 2(a) and one particle is clearly larger than the other three. These three smaller nanoparticles exhibited a higher transmitted intensity contrast when using 633 nm laser, shown in Fig. 2(b). The transmitted intensity contrast became smaller when using 532 nm laser and became the smallest when using 475 nm laser. The decrease in intensity contrast with decreasing excitation wavelength matched the trend shown in the spectrum range between 475 nm and 633 nm of curve (b) in Fig. 1(d). The intensity contrast was the highest when the excitation wavelength was close to the surface plasmon resonance of the Ag nanoparticles. Similar NSOM images of Ag nanoparticles fabricated from 5 nm thin film are shown in Fig. 3. A rectangular area is also high-lighted and three nanoparticles are observed inside this area. The size of the middle nanoparticle is smaller than the other two. NSOM images with different lasers are shown in Fig. 3(b), (c), and (d). These two nanoparticles on the side exhibited the highest intensity contrast when using 475 nm laser. The contrast became smaller with increasing excitation laser wavelength. The decrease in intensity contrast with increasing excitation wavelength matched the trend shown in curve (a) in Fig. 1(d).

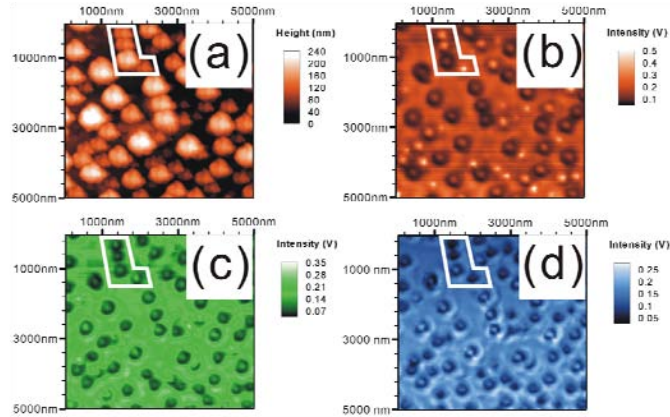


Fig. 2. (a) AFM image and NSOM images taken by using (b) 633 nm, (c) 532 nm, and (d) 475 nm laser light, of Ag nanoparticle fabricated by annealing 10 nm Ag thin film.

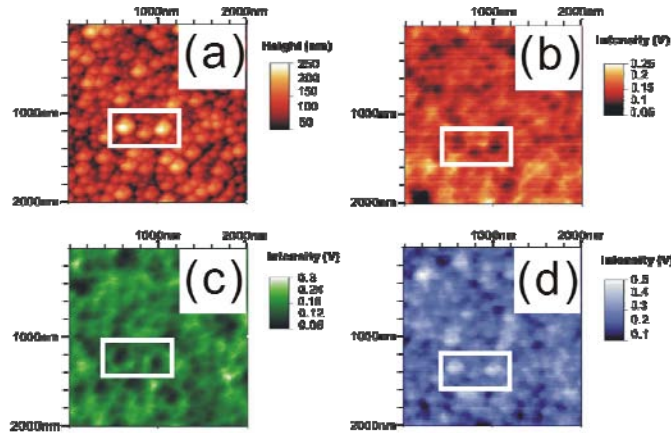


Fig. 3. (a) AFM image and NSOM images taken by using (b) 633 nm, (c) 532 nm, and (d) 475 nm laser light, of Ag nanoparticle fabricated by annealing 5 nm Ag thin film.

From the results shown in Figs. 2 and 3, the intensity contrast for the same Ag nanoparticle depends strongly on the excitation wavelength. The contrast becomes higher when the excitation wavelength is closer to the surface plasmon resonance. For larger Ag nanoparticles, fabricated from 10 nm thin films, the surface plasmon resonance wavelength is close to 630 nm. The strong light scattering of the red laser light ( $\lambda = 633$  nm) by the Ag nanoparticle results in a higher transmitted light intensity from the probe tip and a bright spot in the NSOM image. By moving away from the resonance wavelength, the light scattering becomes weaker and the transmitted light is further reduced due to the blocking by the Ag nanoparticle, which results in a dark spot in the NSOM image. For small Ag nanoparticles, fabricated from 5 nm thin films, the surface plasmon resonance shifts to close to 440 nm. Therefore, the scattering of the Ag

nanoparticle is stronger when using 475 nm light and decrease with increasing wavelength. These results strongly support that surface plasmon resonance scattering can effectively increase the transmitted light intensity from the near-field probe tip. NSOM image of a Ag nanoparticle is a bright spot when the laser wavelength matches its surface plasmon resonance.

To illustrate contrast-enhanced NSOM image of a Ag nanoparticle due to localized surface plasmon resonance, a full 3D finite-difference time-domain (FDTD) simulation was carried out. A Drude-Lorentzian model for the dielectric constant of silver is given as the following

$$\varepsilon(\omega) = \varepsilon_{\infty} - \frac{\omega_D^2}{\omega^2 - j\omega\gamma_D} + \sum_{p=1}^2 \frac{\Delta\varepsilon_p \omega_p^2}{\omega_p^2 + 2j\omega\gamma_p - \omega^2}$$

where  $\omega_D$  is the plasma frequency of the metal and  $\omega_p$  ( $p = 1,2$ ) are the Lorentz resonant frequencies, and  $\gamma$ 's are the damping constants. These parameters were obtained by fitting with the empirical dielectric constant of bulk Ag at wavelengths from 300nm to 800nm [9]. The Ag nanoparticle was modeled as a hemisphere shape due to the thermal annealing process in the experiments. The extinction spectrum of a Ag nanoparticle

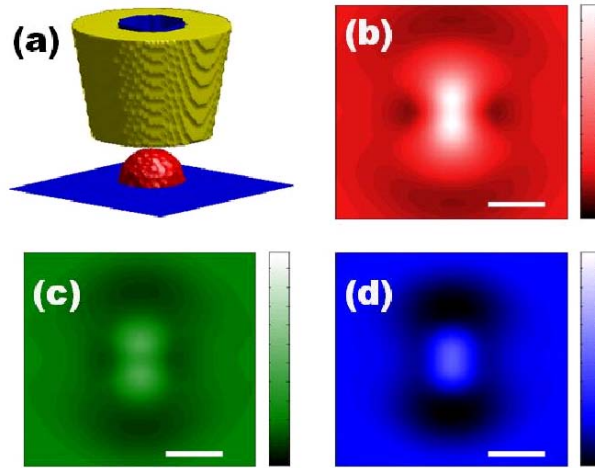


Fig. 4. (a) FDTD simulation geometry shown only for the region near a Ag particle with diameter of 160nm (b) (c) (d) FDTD collected far field intensity pattern from scanning the NSOM tip over a Ag particle at wavelength 632nm, 532nm, 480nm respectively. The intensity is normalized to 1 as the case of no Ag particle. The three color bars all range from [0.5 2.7]. The scale bars indicate 160 nm.

with diameter of 160 nm on a glass substrate was calculated and was shown as the curve (c) in Fig. 1(d). It resembles the absorption spectrum measured in the experiments. To obtain the near-field scanning image of the Ag nanoparticle, a NSOM tip operated at illumination mode was included in the FDTD grid which was similar to an earlier report [10]. The geometry of the region near the Ag nanoparticle is illustrated in Fig. 4(a). By positioning the tip at different locations around the Ag nanoparticle, the integrated far field energy flux was collected as the intensity for each pixel [11]. Three different light sources with wavelengths at 632 nm, 532 nm, and 480 nm were used for two-dimensional scan over an area of 0.6  $\mu\text{m}$  by 0.6  $\mu\text{m}$  around the Ag nanoparticle. The calculated scanning NSOM images at wavelengths 632 nm, 532 nm, 480 nm were shown in Fig. 4(b), (c), and (d), respectively. The color scale was normalized by the background signal when no particle was presented and all three color bars ranged from 0.5 to 2.7. The colors of red, green, and blue were assigned as the background color with color bar value equal to 1. The FDTD results demonstrate a consistent trend that the NSOM image of the Ag nanoparticle became brighter as the probing wavelength moved toward the LSPR peak. These results are consistent with our experimental observation, which indicate that on-resonant metal nanoparticles will enhance the light extraction from the NSOM tip by a factor of at least several times. Depending on the probing light wavelength relative to the LSPR peak of the nanoparticle, the scanning images show drastically difference in contrast. This property is useful for distinguishing nanoparticles of difference sizes and is potential for differentiating nanoparticles of various materials.

## **Conclusion**

Ag nanoparticles fabricated by thermal annealing of Ag thin films were studied using a near-field scanning optical microscopy (NSOM). The transmitted intensity by a NSOM operating at illumination mode was recorded when using light sources with different wavelengths. The transmitted intensity contrast between the Ag nanoparticle and the background is higher when the localized surface plasmon resonance of the Ag nanoparticle matches the wavelength of the light source. This phenomenon is theoretically confirmed by the 3-dimensional finite-difference-time-domain (FDTD) simulations. Therefore, Ag nanoparticles with controlled sizes can be distinguished by NSOM in this study, while conventional atomic force microscopy (AFM) can only

recognize the existence of nanoparticles. By modifying the surface of metal nanoparticles differently according to their sizes, one can obtain a material-specific NSOM images and reveal more material information compared to the current AFM images. Further development of this technique will be beneficial for future nano-imaging of bio-molecular studies.

#### REFERENCES

- [1] U. Durug, D. W. Pohl, and F. Rohner, "Near-field optical-scanning microscopy", *J. Appl. Phys.*, vol. 59, pp. 3318-3327, May 1986.
- [2] J. H. Kim, K. B. Song, "Recent progress of nano-technology with NSOM", *Micron*, vol. 38, pp. 409-426, 2007.
- [3] G. P. Wiederrecht, "Near-field optical imaging of noble metal nanoparticles", *Euro. Phys J. Appl. Phys.*, vol. 28, pp. 3-18, Oct. 2004.
- [4] A. Bouhelier, "Field-enhanced scanning near-field optical microscopy", *Microsc. Res. Tech.*, vol. 69, pp. 563-579, Jul. 2006
- [5] A. Cvitkovic, N. Ocelic, and R. Hillenbrand, "Material-Specific Infrared Recognition of Single Sub-10 nm Particles by Substrate-Enhanced Scattering-Type Near-Field Microscopy", *Nano Lett.*, vol. 7, pp. 3177-3181, Oct. 2007.
- [6] K. L. Kelly, E. Coronado, L. Zhao, G. C. Schatz, "The Optical Properties of Metal Nanoparticles: The Influence of Size, Shape, and Dielectric Environment", *J. Phys. Chem. B*, vol. 107, pp. 668-677, Jan. 2003.
- [7] T. Klar, M. Perner, S. Grosse, G. Von Plessen, W. Spirkl, and J. Feldmann, "Surface-plasmon resonances in single metallic nanoparticles", *Phys. Rev. Lett.*, vol. 80, pp. 4249-4252, May 1998.
- [8] S. Benrezzak, P. M. Adam, J. L. Bijeon, and P. Royer, "Observation of nanometric metallic particles with an apertureless scanning near-field optical microscope", *Sur. Sci.*, vol. 491, pp. 195-207, Sep. 2001.
- [9] T. W. Lee, and S. K. Gray, "Subwavelength light bending by metal slit structures", *Opt. Express*, vol. 13, pp. 9652-9659, Nov. 2005.
- [10] S. -H. Chang, S. K. Gray, and G. C. Schatz, "Surface plasmon generation and light transmission by isolated nanoholes and arrays of nanoholes in thin metal films", *Opt. Express*, vol. 13, pp. 3150-3165, Apr. 2005.
- [11] E. -S. Kwak, J. Henzie, S. -H. Chang, S. K. Gray, G. C. Schatz, and T. W. Odom, "Surface plasmon standing waves in large-area subwavelength hole arrays", *Nano Lett.*, vol. 5, pp. 1963-1967, Oct. 2005.

## **V. Future work**

In this research, metallic nanoparticles were fabricated using thermal annealing and Nanosphere lithography. We have systematically study the surface plasmon resonance frequency for different metal nanoparticle with different sizes. After the establishments of these data bases, we will be able to find the best solar cell materials and integrate the cell design with the selected metal nanoparticles. We are in the progress to integrate the metallic nanoparticle arrays with organic solar cells. Our future work will be to finish the integration process and analyzed the fabricated solar cells with standard solar cell characterization.

In addition, we have developed the nanofabrication capability using Nanosphere Lithography. The technique is fast and economic, which will be very attractive for current industrial applications. Therefore, we will further investigate this technique and search for new applications that will greatly improve the implementation of nanotechnology into the industry.

Finally, the knowledge we gained from this research will also be beneficially for other photonic applications, e.g. LED technology. The plasmonic-enhanced LED design will also be very important for the future solid-state lighting application.

## **VI. Conclusions**

In conclusion, metallic nanoparticles fabricated using thermal anneal and Nanosphere lithography were achieved in the research. Surface plasmon resonances of different metallic nanoparticles were both experimentally and theoretically studied. Data bases related to the plasmonic resonance for different metal were established. The integration of selected metal nanoparticles and organic thin film were successfully achieved. The standard solar cell electric characterizations are currently under investigation. Near-field Scanning Optical Microscopy (NSOM) were used to investigated the near-field electric field of the metal nanoparticles when using light that was resonant to the metal nanoparticles. Great electric fields were detected by the used of NSOM and help to understand the effects of surface plasmon of metal nanoparticles. The future work includes the integration of metal nanoparticle into several solar cell applications. In addition, the development of Nanosphere lithography will also be beneficial for future nanofabrication application. The results from this research have already established the cornerstone for further research on the plasmonic-enhanced photonic devices, including solar cell and light-emitting devices. The enhanced performance for these optoelectronic devices will have great impact for the development of future technologies.